

Space-Fractional Diffusion with a Potential Power-Law Coefficient: Transient Approximate Solution

Jordan Hristov*

Department of Chemical Engineering, University of Chemical Technology and Metallurgy, Sofia, Bulgaria.

Received: 11 Jul. 2016, Revised: 24 Nov. 2016, Accepted: 29 Nov. 2016

Published online: 1 Jan. 2017

Abstract: An approximate analytical solution of transient diffusion equation with space-fractional Riemann–Liouville fractional derivative has been developed. The integral-balance method and an assumed parabolic profile with undefined exponent have been used. The spatial correlation the superdiffusion coefficient in potential power-law form has been discussed. The laws of the spatial and temporal propagation of the solution are the primary issues. Approximate solutions based on assumed parabolic profile with unspecified exponent have been developed.

Keywords: Approximate analytical solution, integral-balance method, spatial-fractional diffusion equation.

1 Introduction

1.1 The superdiffusion model

Fractional differential equations (FDEs) are suitable for modelling of anomalous diffusive processes in physics [1], porous media [2], plasma flow [3] and turbulence [4]. Analytical solutions for FDEs are not very popular in the literature [5,6,7,8,9,10,11,12] but the methods applied avoid effective engineering analyzes, and therefore, numerical methods are frequently applied [13,14,15,16,17].

This article considers 1-D non-linear space-fractional equation of order $1 < \beta < 2$ and a potential power-law diffusion coefficient $D_\beta [m^\beta / s]$:

$$\frac{\partial u(x,t)}{\partial t} = D_\beta(x) \frac{\partial^\beta u(x,t)}{\partial x^\beta}, \tag{1}$$

$$D_\beta(x) = D_{\beta 0} + \gamma x^\alpha, \alpha \leq \beta, x \geq 0, D_{\beta 0} > 0, \gamma \geq 0, \tag{2}$$

where the space-fractional derivative in $\partial^\beta u(x,t) / \partial x^\beta$ in Eq.(1) is either of Riemann-Liouville (RL) (3) or Caputo type (4) of order β ($1 < \beta < 2$) [18]

$$\frac{\partial^\beta u(x,t)}{\partial x^\beta} =_{RL} D_\beta^x = \frac{1}{\Gamma(2-\beta)} \frac{d^2}{dx^2} \int_0^x \frac{u(x,t)}{(x-z)^{\beta-1}} dz, \tag{3}$$

$$\frac{\partial^\beta u(x,t)}{\partial x^\beta} =_C D_\beta^x = \frac{1}{\Gamma(2-\beta)} \int_0^x \frac{1}{(x-z)^{\beta-1}} \frac{d^2 u(x,t)}{dx^2} dz, \tag{4}$$

$$\frac{\partial^\beta u(x,t)}{\partial x^\beta} = \frac{\partial^2 u(x,t)}{\partial x^2}, \beta = 2. \tag{5}$$

As mentioned above numerical methods [19,20,21,22,23,24,25] dominate in the literature while analytical solutions are rare [26,27,28,29,30,31]. In the context of the solution developed in this work it is worthy to note that fundamental

* Corresponding author e-mail: jordan.hristov@mail.bg

solutions of the time-space and especially the space-fractional equation (1) has been developed in [29] using Green functions and the similarity variable $\xi = x/(Dt)^{1/\beta}$. Therefore, it is a challenging task to develop analytical solutions which would allow straightforward physical analyzes an to be suitable for engineering applications.

1.2 The superdiffusion coefficient $D_\beta(x)$ and its physically correct spatial correlation

Before starting the formulation of the problem for the solution we have to stress the attention on the expressions presenting the spatial dependence of $D_\beta(x)$ as an important issue related to the physical adequacy of the model represented by (1) and (2). The superdiffusivity coefficient $D_\beta(x) = D_{\beta 0}x^\alpha$ is commonly used in numerical examples demonstrating various solution approaches to (1) [28,32]. The common approached is to present (2) as $D_\beta(x) = \Gamma(*)x^\alpha$, a form usually chosen to handle numerical or analytical solutions [26,27,28,29,32], where $\Gamma(*)$ is the Euler Gamma function. However, both sides of (1) should have equal dimensions only when the coefficient D_β has a dimension of m^β/s . In the case of constant (space-independent) diffusivity the expression is correct, but with (2) the dimension of $D_{\beta 0}$ should be $1/s$ in order (1) to be dimensionally homogeneous. It is obvious that the expression of $D_{\beta 0}$ as $\Gamma(*)$ does not meet this requirement since it is dimensionless, but actually this is not an obstacle to perform mathematical exercises [28,32]. Moreover at $x = 0$ we have $D_\beta(x = 0) = 0$ and we see that (1) degenerates. Actually, if we have to calculate the flux at the boundary $x = 0$ expressed as $q = -D_\beta(0)[\partial^\beta u(0,t)/\partial x^\beta]$ the physical inadequacy appears immediately because the transport coefficient $D_\beta(x)$ cannot be zero everywhere in the medium. Since the superdiffusivity cannot be zero at the boundary an alternative form of the spatial approximation of $D_\beta(x)$ is suggested here as.

$$D_\beta(x) = D_{\beta 0} + \gamma_x x^\alpha \Rightarrow D_\beta(x) = D_{\beta 0}(1 + k_x x^\alpha), 0 \leq x \leq \infty. \quad (6)$$

The dimension of γ_x is $m^{\beta-\alpha}/s$ because the entire expression of $D_\beta(x)$ should have a dimension m^β/s ; respectively the dimension of $k_x = \gamma_x/D_{\beta 0}$ is $1/m^\alpha$. It is noteworthy that the expressions (2) and (6) are common in the integer-order models of diffusion and heat conduction [33,34,35,36] and termed as potential power-law diffusivity. Especially the form (6) has not been observed as a modelling approach in the published literature. The present study addresses both forms of $D_\beta(x)$ expressed by (2) and (6).

1.3 Aim and paper organization

The work demonstrates how by application of the integral-balance approach [37,38,39,40,41] an approximate analytical solutions of the space-fractional equation eq.(1) in case of the Dirichlet problem and Riemann-Liouville space-fractional derivative can be developed.

The article is organized as follows: Section 2 develops the solution of the Dirichlet problem through application of the integral balance approach. Section 2.3 demonstrates how the spatial integration of the fractional derivative resulting in the general expressions of the penetration depths can be developed. Section 2.4 develops approximate evaluation of the integrals of the approximate space-fractional derivative by expressing of the approximate profile as a truncated convergent series. Section 2.5 considers the restrictions imposed on the exponent of the profile at the boundary of the penetration layers and the conditions required positive values of the expressions through the truncated series to be assured. Section 2.6 applied the least-squares method for refining the approximate solution and determination of the optimal exponents of the parabolic profile. Section 2.7 present numerical simulations with the developed approximate solutions and relevant physical comments.

2 Dirichlet Problem

2.1 The Integral-balance approach

Consider eq.(1) with initial and boundary conditions

$$u(x, 0) = 0, u_x(x, 0) = 0, u(0, t) = 1, u(\infty, t) = 0, t \geq 0. \quad (7)$$

The integral-balance method is based on a finite sharp front $\delta(t)$ concept thus allowing the boundary condition $u(\infty, t) = 0$ to be re-defined as

$$u(0) = 1, u(\delta) = \frac{\partial u(\delta, t)}{\partial x} = 0. \quad (8)$$

The integration over the penetration depth results in

$$\int_0^\delta \frac{\partial u(x,t)}{\partial t} dx = \int_0^\delta D_\beta(x) \frac{\partial^\beta u(x,t)}{\partial x^\beta} dx. \tag{9}$$

Now, applying the Leibniz rule to (9) we get

$$\frac{d}{dx} \int_x^\delta u(x,t) dx = \int_0^\delta D_\beta(x) \frac{\partial^\beta u(x,t)}{\partial x^\beta} dx. \tag{10}$$

Further, by replacement of $u(x,t)$ by an approximate function $u_a = u_a(x/\delta)$ expressed through the dimensionless space variable $\eta = x/\delta$, where $0 < x/\delta < 1$ the penetration depth $\delta(t)$ can be defined.

2.2 Assumed profile and the spatial scale transform

An assumed parabolic profile with unspecified exponent [38,39,40,41] is used, namely

$$u_a(x) = \left(1 - \frac{x}{\delta}\right)^n. \tag{11}$$

This profile satisfies the conditions (8) and forms two zones: $u_a(x) > 0$ for $x < \delta$ and $u_a(x) = 0$ for $x \geq \delta$. The solution based on the assumed profile (11) requires $n > 0$ which should depend on the fractional order β .

To be correct in the evaluation of $\partial^\beta u_a(x)/\partial x^\beta$ we change the variable in (1) as $\eta = x/\delta$ where $0 \leq \eta \leq 1$. That is, $u_a(x) \Rightarrow F_a(1 - \eta) = (1 - \eta)^n$ and after the scale change $x \rightarrow \eta$ the space-fractional derivative of the assumed profile can be presented as:

$$\frac{\partial^\beta u_a(x)}{\partial x^\beta} = \left(\frac{1}{\delta}\right)^\beta \frac{\partial^\beta F_a(\eta)}{\partial \eta^\beta}. \tag{12}$$

Further, the right-hand side of (1) with $D_\beta(x) = D_{\beta 0} + \gamma_x x^\alpha$ can be presented as

$$(D_{\beta 0} + \gamma_x x^\alpha) \frac{1}{\delta^\beta} \frac{\partial^\beta F_a(\eta)}{\partial \eta^\beta} = D_{\beta 0} \delta^{-\beta} \frac{\partial^\beta F_a(\eta)}{\partial \eta^\beta} + \gamma_x \eta^\alpha \delta^{\alpha-\beta} \frac{\partial^\beta F_a(\eta)}{\partial \eta^\beta}. \tag{13}$$

2.3 Spatial integration and the penetration depth

Now, we turn on the integration of the fractional derivative in (9) using $u_a(x,t)$ instead $u(x,t)$. Precisely, in terms of the dimensionless variable $\eta = x/\delta$ (changing the variable in the integral as $x \rightarrow \eta = x/\delta$ we get

$$\int_0^\delta D_\beta(x) \frac{\partial^\beta u_a(x,t)}{\partial x^\beta} dx = \int_0^1 D_\beta(x) D_{\beta 0} \delta^{1-\beta} \frac{\partial^\beta F_a(\eta)}{\partial \eta^\beta} d\eta + \int_0^1 \gamma_x \eta^\alpha \delta^{1+\alpha-\beta} \frac{\partial^\beta F_a(\eta)}{\partial \eta^\beta} d\eta. \tag{14}$$

Next, the integration of in left side of (9) from 0 to δ with the assumed profile gets

$$\frac{d}{dt} \int_0^\delta u_a(x,t) dx = \frac{d}{dt} \int_0^\delta \left(1 - \frac{x}{\delta}\right)^n dx = \frac{1}{n+1} \frac{d\delta}{dt}. \tag{15}$$

Now, we have to see how the integral-balance relation (9) through the assumed profile (11) provides equations about the propagation of the front $\delta(t)$.

2.3.1 Penetration depth

The integral-balance relation, taking into account the previous results (see (14) and (15)) and replacing $u(\eta)$ by $F_a(\eta) = (1 - \eta)^n$, yields

$$\frac{1}{n+1} \frac{d\delta}{dt} = D_{\beta 0} \delta^{1-\beta} \int_0^1 \frac{\partial^\beta F_a(\eta)}{\partial \eta^\beta} d\eta + \gamma_x \delta^{1+\alpha-\beta} \int_0^1 \eta^\alpha \frac{\partial^\beta F_a(\eta)}{\partial \eta^\beta} d\eta. \tag{16}$$

$$\frac{1}{n+1} \frac{d\delta}{dt} = D_{\beta 0} \delta^{1-\beta} \Phi_0(n, \alpha, \beta) + \gamma_x \delta^{1+\alpha-\beta} \Phi_1(n, \alpha, \beta). \quad (17)$$

$$\Phi_0(n, \alpha, \beta) = \int_0^1 \frac{\partial^\beta F_a(\eta)}{\partial \eta^\beta} d\eta. \quad (18)$$

Equation (17) is a non-linear ODE of Bernoulli type and a direct solution through the classical approach using integrating factor is impossible since we try to solve it in a general manner, not with specified values of β and α . We will use two alternative approaches based on preceding solutions of space fractional diffusion equation [42,43], namely

Approach 1 Equation (17) can be re-arranged as

$$\frac{1}{\beta(n+1)} \frac{d\delta^\beta}{dt} = D_{\beta 0} \Phi_0(n, \alpha, \beta) + \delta^\alpha \gamma_x \Phi_1(n, \alpha, \beta). \quad (19)$$

Denoting $\delta^\beta = y$, that means $\delta^\alpha = y^{\alpha/\beta}$ we get a non-linear ODE

$$\frac{dy}{dt} = a + by^p, \quad p = \frac{\alpha}{\beta}, \quad (20)$$

$$a = D_{\beta 0} \beta(n+1) \Phi_0(n, \alpha, \beta), \quad b = \gamma_x \beta(n+1) \Phi_1(n, \alpha, \beta). \quad (21)$$

Further we suggest that $y = \delta^\beta = \lambda t$ which intuitively comes from the solution with a constant superdiffusivity $D_\beta = D_{\beta 0}$ [42]. The relationship $\delta^\beta = y = \lambda t$ satisfies the initial condition $\delta^\beta(0) = y(0) = 0$ and the factor λ should be determined through the solution. Then, with this substitution we get $\delta^\alpha = y^{\alpha/\beta} = y^p = \lambda^p t^p$ and consequently (17) can be re-written as

$$\frac{dy}{dt} = a + b\lambda^p t^p. \quad (22)$$

The Laplace transform of (22) is

$$sY(s) = \frac{a}{s} + \frac{b\lambda^p}{s^{1+p}} \Gamma(1+p) \implies Y(s) = \frac{a}{s^2} + \frac{b\lambda^p}{s^{1+(1+p)}} \Gamma(1+p). \quad (23)$$

The inverse Laplace transform of (23) results in

$$y(t) = at + b\lambda^p t^{1+p} \frac{\Gamma(1+p)}{\Gamma(2+p)} \implies y(t) = at + b\lambda^p t^{1+p} \frac{1}{1+p}. \quad (24)$$

Therefore, explicitly the penetration depth is

$$\delta = \left(at + \frac{b\lambda^p}{(1+\alpha/\beta)} t^{1+\frac{\alpha}{\beta}} \right)^{\frac{1}{\beta}} \implies \delta_1 = (at)^{\frac{1}{\beta}} \left[1 + \frac{b}{a} \lambda^p \frac{1}{(1+\alpha/\beta)} t^{\frac{\alpha}{\beta}} \right]^{\frac{1}{\beta}}. \quad (25)$$

For $b = 0$ we get the solution with the constant diffusion coefficient [42] Now, we turn on the definition of the factor λ . Since δ is the penetration distance with a dimension of length m then the large term in squared brackets of δ_1 (see (25)) should be dimensionless, that is, the ratio $b\lambda^p/a$ should have a dimension $s^{-\alpha/\beta}$. Reasonably λ^p should have a dimension $m^\alpha/s^{\alpha/\beta}$ and consequently λ gets the dimension m^β/s that matches the superdiffusion coefficient $D_{\beta 0}$. Therefore, the substitution $y = \delta^\beta = \lambda t$ is equivalent to $\delta^\beta = D_{\beta 0} t$, which a particular solution of the linear case ($\alpha = 0$) [42], as mentioned above.

Approach 2 Dividing both sides of Eq. (17) by $\delta^{1+\alpha-\beta}$ one obtain

$$\frac{d\delta}{dt} = c\delta^{-\alpha} + d, \tag{26}$$

$$c = (\beta - \alpha)D_{\beta 0}\Phi_0(n, \alpha, \beta), d = (\beta - \alpha)D_{\beta 0}\Phi_1(n, \alpha, \beta). \tag{27}$$

Denoting $\delta^{\beta-\alpha} = z$ that means $\delta^{-\alpha} = z^{\alpha/(\alpha-\beta)} = z^k$, where $k = -\alpha/(\beta - \alpha)$ we may express (26) as a Bernoulli equation

$$\frac{dz}{dt} = cz^k + d. \tag{28}$$

Further, we suggest that $z = \mu.t$ which intuitively comes from the solution with a power-law superdiffusivity [43] and corresponding to second term in the right-hand side of the extended equation (13). The relationship $\delta^{\beta-\alpha} = z = \mu.t$ satisfies the initial condition $\delta^{\beta-\alpha}(0) = z(0) = 0$ and the factor μ should be determined through the solution. Then, with this substitution we get $\delta^{-\alpha} = z^{-\alpha/(\beta-\alpha)} = z^k = \mu^k t^k$ and consequently eq. (28) can be re-written as

$$\frac{dz}{dt} = d + c\mu^k t^k. \tag{29}$$

The Laplace transform of (29) is

$$sZ(s) = \frac{d}{s} + \frac{c\mu^k}{s^{1+k}}(1+k) \implies Z(s) = \frac{d}{s^2} + \frac{c\mu^k}{s^{1+(1+k)}}\Gamma(1+k). \tag{30}$$

The inverse Laplace transform of (30) results in

$$z(t) = dt + c\mu^k t^k \frac{1}{1+k} \implies \delta^{\beta-\alpha} = dt + c\mu^{-\alpha/(\beta-\alpha)} t^{-\alpha/(\beta-\alpha)} \frac{1}{1-\alpha/(\beta-\alpha)}. \tag{31}$$

Hence, we may express the penetration depth in a way similar to (25)

$$\delta_2 = (dt)^{\frac{1}{\beta-\alpha}} \left[1 + \frac{c}{d} \mu^k \frac{1}{1-\alpha/(\beta-\alpha)} t^{\frac{-\alpha}{\beta-\alpha}} \right]^{\frac{1}{\beta-\alpha}}. \tag{32}$$

Now, we turn on the definition of the factor μ in a way already used in Approach 1. Since δ is the penetration distance with a dimension of length we may easy check that $(dt)^{1/(\beta-\alpha)} \propto (y_x t)^{1/(\beta-\alpha)}$ has dimension of length because by definition the dimensions of γ_x is $m^{\beta-\alpha}/s$. Therefore, the term in the squared bracket of (32) should be dimensionless. The product $\mu^k(c/d) = \mu^k(D_{\beta 0}/\gamma_x)$ should have a dimension s^{-k} . Precisely, the ratio $D_{\beta 0}/\gamma_x^{1-k}$ defines a time scale of the process as it will be commented in the next section. Therefore, the substitution $\delta^{\beta-\alpha} = z = \mu t$ is equivalent to $\delta^{\beta-\alpha} = \gamma_x t$, which is a particular solution of the case with the power-law diffusivity $D_\beta = D_{\beta 0} x^\alpha$ [43], as mentioned above.

2.3.2 The fractional time scale and the definition of the ${}_s H_r$ number

The solution about $\delta(t)$ in the form (25) allows defining the fractional quasi-Fourier number in the following way. Since $\lambda = D_{\beta 0}$ then the ratio $b/a = (\gamma_x/D_{\beta 0}^{1-\alpha/\beta})(\Phi_1/\Phi_0)$ is a scaled characteristic time of the fractional diffusion process defined as $t_1^{\alpha/\beta} = D_{\beta 0}^{1-\alpha/\beta}/\gamma_x$ with a dimension $[s^{\alpha/\beta}]$. Precisely, the characteristic time is $t_1 = (D_{\beta 0}^{1-\alpha/\beta}/\gamma_x)^{\beta/\alpha}$. Therefore, the ratio $t^{\alpha/\beta}/t_1^{\alpha/\beta} = (b/a)\lambda^{\alpha/\beta} t^{\alpha/\beta}/t_0 = {}_s H_r$ is a scaled fractional quasi-Fourier number for the case of potential power-law superdiffusivity (6). With more details, in terms of the process parameters the fractional quasi-Fourier number ${}_s H_r$ can be defined as

$${}_s H_r = t \left(\frac{\gamma_x}{D_{\beta 0}^{1-\alpha/\beta}} \right)^{-\beta/\alpha}. \tag{33}$$

The lower prefix s means *space*. In contrast, with the power-law diffusivity $D_\beta(x) = D_{\beta 0}x^\alpha$ [43] such a definition is impossible since in the semi-infinite medium at issue, *there is no physically defined characteristic length scale*. The advantage of the definition (6) is its physical adequacy and the ability to present the penetration depth (see eq.(33)) as

$$\delta_1 = (at)^{\frac{1}{\beta}} \left[1 + (sH_r)^{\frac{\alpha}{\beta}} \frac{\Psi(n, \alpha, \beta)}{1 + \alpha/\beta} \right]^{\frac{1}{\beta}}. \quad (34)$$

$$\Psi(a, \alpha, \beta) = \frac{\Phi_1(n, \alpha, \beta)}{\Phi_0(n, \alpha, \beta)}. \quad (35)$$

Now, with $a = D_{\beta 0}\beta(n+1)\Phi_0(n, \alpha, \beta)$ from eq.(21) we have

$$\delta_1 = (D_{\beta 0}t)^{\frac{1}{\beta}} (\beta(n+1)\Phi_0(n, \alpha, \beta))^{\frac{1}{\beta}} \left[1 + (sH_r)^{\frac{\alpha}{\beta}} \frac{\Psi(n, \alpha, \beta)}{1 + \alpha/\beta} \right]^{\frac{1}{\beta}}. \quad (36)$$

Therefore, the contribution of the second term of the superdiffusivity to the evolution of the penetration depth depends on the ratio $D_{\beta 0}^{1-\alpha/\beta}/\gamma_s$ and its growth is proportional to $t^{\alpha/\beta}$ (see (25) or $t^{1/(\beta-\alpha)}$). Since for $\alpha/\beta < 1$ the growth in time of the second terms of (25) and ((36) is slower than that of the factors $(D_{\beta 0}t)^{1/\beta}$ and $(\gamma_s t)^{1/(\beta-\alpha)}$ which actually dominate the superdiffusion process.

Similarly, with Approach 2 and the final expression (32) we define an alternative characteristic time scale t_2 , which in terms of the process parameters is presented as (37) and (38), namely

$$\frac{c}{d} \mu^k t^{\frac{-\alpha}{\beta-\alpha}} = \left(\frac{D_{\beta 0}}{\gamma_x} \right) t^k = \frac{t^k}{t_2^k}, \quad (37)$$

$$t_2 = \left(\frac{D_{\beta 0}}{\gamma_x^{1-k}} \right)^{\frac{1}{k}} = \frac{\gamma_x^{\beta/\alpha}}{D_{\beta 0}^{(\beta-\alpha)/\alpha}} = \left(\frac{\gamma_x^\beta}{D_{\beta 0}^{(\beta-\alpha)}} \right)^{\frac{1}{\alpha}}. \quad (38)$$

Consequently, the ratio defined by (37) can be considered as a scaled quasi-fractional Fourier number $(sH_{r_2})^k = (t/t_2)^k$. Therefore, we may express the penetration depth in two alternative forms, namely

$$\delta_2 = (\gamma_x t)^{\frac{1}{\beta-\alpha}} [(\beta-\alpha)\Phi_1(n, \alpha, \beta)]^{\frac{1}{\beta-\alpha}} \left[1 + (sH_{r_2})^{\frac{-\alpha}{\alpha-\beta}} \frac{1}{\Psi(n, \alpha, \beta)[1 - \alpha/(\beta-\alpha)]} \right]^{\frac{1}{\beta-\alpha}}. \quad (39)$$

$$\delta_2 = (\gamma_x t)^{\frac{1}{\beta-\alpha}} \left[(\beta-\alpha)\Phi_1(n, \alpha, \beta)^{\frac{1}{\beta-\alpha}} + (sH_{r_2})^{\frac{-\alpha}{\alpha-\beta}} \frac{(\beta-\alpha)\Phi_0(n, \alpha, \beta)}{[1 - \alpha/(\beta-\alpha)]} \right]^{\frac{1}{\beta-\alpha}}. \quad (40)$$

However, the above definitions of sH_{r_1} and sH_{r_2} raise the question: what is the difference between them and how to proceed further in the calculations? The answer is straightforward. Since $sH_{r_1} = t/t_1$ and $sH_{r_2} = t/t_2$ then the ratio $sH_{r_1}/sH_{r_2} = t_1/t_2$, i.e. the ratio of the time scales. From the definitions of t_1 and t_2 we get

$$\frac{sH_{r_1}}{sH_{r_2}} = \frac{t_2}{t_1} = \frac{\gamma_\beta^x/\alpha}{D_{\beta/\alpha}^{\beta 0} - 1} = 1$$

Therefore, the two definitions are identical, i.e. $sH_{r_1} = sH_{r_2} = sH_r$. We will use further only the symbol sH_r .

2.3.3 The penetration front propagation and related conditions imposed on the exponent α

It is clear that the values of α and β control the behavior of the diffusion processes and therefore it is quite important to see the mechanism through which the solution controlled by α and β can delineate two principle regimes of superdiffusion.

Fast superdiffusion It is noteworthy that the result (36) strictly defines the condition to be satisfied since the physics dictates a growing in time penetration depth. Now, we stress the attention on the result (40) where the effect of the interrelation of the exponents α and β is more clear. If for fixed value of β the exponent α will increase then the exponent $1/(\beta - \alpha)$ will increase, that is a fast propagation in time will take place. Oppositely, for decreasing α the exponent $1/(\beta - \alpha)$ will decrease and diffusion will be performed slower. That is, the fast subdiffusion process corresponds to increasing α within the range $0 \leq \alpha \leq 1$ because by definition we have $1 < \beta < 2$.

Moreover, the speed of the penetration front is $d\delta/dt \propto (1/(\beta - \alpha))t^{(1+\alpha-\beta)/(\beta-\alpha)}$. The condition $1 + \alpha - \beta > 0$ (together with $\beta > \alpha$) assures an increasing in time speed of the penetration front. Precisely, this means $\alpha > \beta - 1$. If $\beta = 1.1$, for instance, then the positive growth of the penetration depth needs $0.1 < \alpha < 1$ or when $\beta = 1.5$, the condition is $0.5 < \alpha < 1$. Further, for specific case of $\alpha = 0$ (constant coefficient of super diffusivity) the speed of the front is $d\delta/dt \propto (1/\beta)t^{(1-\beta)/\beta}$ and because the ratio $(1 - \beta)/\beta$ is always negative, the front will propagate with a speed decaying in time.

For the intermediate case $\alpha = \beta - 1$, the penetration front propagates linearly in time, i.e. $\delta(t) = (\gamma_x t)(n + 1)\Phi_1(n, \alpha, \beta)$ with a constant speed defined as $d\delta/dt = D_{\beta 0}(n + 1)\Phi_1(n, \alpha, \beta)$. For $\alpha = \beta$ we get $\delta = 0$ and a blow-up of the speed. However, such a situation is impossible because the above estimates indicate that $0 \leq \alpha \leq 1$ and $1 < \beta < 2$. The present work is restricted to situation where $0 \leq \alpha \leq 1$ in order to elucidate in better way the retardation factor of the fractional order β .

All these cases will be discussed further in the analysis of the approximate solutions with respect to the type of anomalous diffusion process modeled depending on the difference $(\beta - \alpha)$.

Slow superdiffusion The expression (39) about the penetration depth δ_2 , without lost of generality, for $\alpha < 0$, but with $1 < \beta < 2$ (in order to match the situation with the fast superdiffusion) can be re-written as

$$\delta_p(t) \equiv (D_{\beta 0}t)^{\frac{1}{\beta+\alpha}} [(\beta + \alpha)(n + 1)\Phi_1(n, \alpha, \beta)]^{\frac{1}{\beta+\alpha}}. \tag{41}$$

If for fixed value of β , the absolute value of α increases then the exponent $1/(\beta + \alpha)$ decreases; that is the diffusion process will decelerate. Oppositely, if the absolute value of α decreases, the penetration the time growth of δ will be faster. That is, the *slow superdiffusion process* corresponds to increasing absolute value of α when $\alpha < 0$. Referring to the case with $\alpha = 0$ when the spatial damping effect depends only on the value of the fractional order β we have the case of *slow spatial superdiffusion*. Subsequently, with $\alpha > 0$ (fast spatial superdiffusion) the diffusant will penetrate faster into the medium. Oppositely, for $\alpha < 0$ (slow spatial superdiffusion) the diffusion will be slower than in the case with $\alpha = 0$.

2.3.4 Approximate profiles (solutions)

After determination of the penetration depths by the integral-balance method the approximate solutions are

$$u_{a1} = \left(1 - \frac{x}{(D_{\beta 0}t)^{\frac{1}{\beta}} N_1}\right)^n = \left(1 - \frac{\xi_1}{N_1}\right)^n, \tag{42}$$

$$N_1 = [(\beta)(n + 1)\Phi_0(n, \alpha, \beta)]^{\frac{1}{\beta}} \left[1 + ({}_s Hr)^{\frac{\alpha}{\beta}} \frac{\Psi(n, \alpha, \beta)}{(1 + \alpha/\beta)}\right]^{\frac{1}{\beta}}. \tag{43}$$

$$u_{a2} = \left(1 - \frac{x}{(\gamma_x t)^{\frac{1}{\beta-\alpha}} N_2}\right)^n, \tag{44}$$

$$N_2 = \left[(\beta - \alpha)\Phi_1(n, \alpha, \beta)^{\frac{1}{\beta-\alpha}} + ({}_s Hr)^{\frac{-\alpha}{\beta-\alpha}} \frac{(\beta - \alpha)\Phi_0(n, \alpha, \beta)}{[1 - \alpha/(\beta - \alpha)]}\right]^{\frac{1}{\beta-\alpha}}. \tag{45}$$

These approximate solutions define in a natural way the similarity variables $\xi_1 = x/(D_{\beta 0}t)^{1/\beta}$ and $\xi_2 = x/(\gamma_x t)^{1/(\beta-\alpha)}$.

2.4 Evaluation of $\Phi_0(n, \alpha, \beta)$, $\Phi_1(n, \alpha, \beta)$ and $\Psi(n, \alpha, \beta)$

The evaluation of $\Phi_0(n, \alpha, \beta)$ and $\Phi_1(n, \alpha, \beta)$ will be carried out by expansion of $F(\eta) = (1 - \eta)^n$ as a convergent series (expressed as a finite sum), namely

$$F_a(\eta) = (1 - \eta)^n \approx \sum_{j=0}^K m_j \eta^j, m_j = \frac{F_a^{(j)}(0)}{\Gamma(j+1)}, 0 < \eta < 1. \quad (46)$$

The fractional integration of (46) (Ref.[44]–p. 70) results in

$$\frac{\partial^\beta F_a(x)}{\partial \eta^\beta} = {}_{RL}D_x^\beta \approx \sum_{j=0}^K \frac{m_j}{\Gamma(j - \beta + 1)} \eta^{1-\beta} = \eta^{-\beta} \sum_{j=0}^K \frac{m_j}{\Gamma(1 - \beta + 1)} \eta^j. \quad (47)$$

Particularly, if the Caputo derivative is used, then same operation applied to (46) yields

$$\frac{\partial^\beta F_a(x)}{\partial \eta^\beta} = {}_C D_x^\beta \approx \sum_{j=1}^K \frac{m_j}{\Gamma(j - \beta + 1)} \eta^{j-\beta}. \quad (48)$$

Hence, the only difference is the first term comparing to (47). The series (47) converges [44], that can be easily checked through the ratio test. Further, integrating the series (46) from 0 to 1 we get the approximation of $\Phi_0(n, \alpha, \beta)$, that is

$$\Phi_0(n, \alpha, \beta) \approx \int_0^1 \sum_{j=0}^K \frac{m_j}{\Gamma(j - \beta + 1)} \eta^{1-\beta} d\eta \approx \sum_{j=0}^K \frac{m_j}{\Gamma(2 + j - \beta)}. \quad (49)$$

Further, using the result (47) we calculate

$$\varphi_1 = \eta^\alpha \frac{\partial^\beta F_a(\eta)}{\partial \eta^\beta} = {}_{RL}D_x^\beta \approx \sum \frac{m_j}{\Gamma(j - \beta + 1)} \eta^{j-\beta+\alpha}. \quad (50)$$

Then,

$$\Phi_1(n, \alpha, \beta) = \int_0^1 \varphi_1 d\eta = \sum_{j=0}^K \frac{m_j}{(j - \beta + \alpha + 1)\Gamma(j - \beta + 1)}. \quad (51)$$

Now, we get

$$\Psi(n, \alpha, \beta) = \sum_{j=0}^K \frac{m_j}{(j - \beta + \alpha + 1)\Gamma(j - \beta + 1)} \left(\sum_{j=0}^K \frac{m_j}{\Gamma(2 + j - \beta)} \right)^{-1}. \quad (52)$$

2.5 Restrictions on the exponent of the profile and ranges of variations

2.5.1 Behavior of the exponent n at the boundaries and restrictions thereof

The integral-balance method define the form of the approximate solution (11) by definition of the functional relationship of $\delta(t)$ as function of the exponent n . However, the boundary conditions imposed by the integral method are not sufficient to be define (8) [41, 45]. Hence, a refining method with already defined function (approximate solution) has to be applied. At this point we apply the least-squares method where the residual function of (1) is

$$R(u_a(x, t)) = \frac{\partial u(x, t)}{\partial t} - D_\beta(x) \frac{\partial^\beta u(x, t)}{\partial x^\beta}. \quad (53)$$

The function $R(u_a(x, t))$ should be equal to zero if u_a is the exact solution but with approximate profile we should look for a minimum thus defining the exponent n . With $u_a = (1 - x/\delta)^n = F_a(\eta)$ we have

$$R(u_a(x, t)) = n(1 - \eta)^{n-1} \frac{n}{\delta} \frac{d\delta}{dt} - D_{\beta 0} \delta^{-\beta} \frac{\partial^\beta F_a(\eta)}{\partial \eta^\beta} - \gamma_\alpha \delta^{\alpha-\beta} \frac{\partial^\beta F_a(\eta)}{\partial \eta^\beta}. \quad (54)$$

At the boundary $x = 0 = \eta = 0$ we have $R(u_a(x, t)) = 0$ for any n and therefore additional constraints cannot be defined.

Further, at the vicinity of the front, that is for $x \rightarrow \delta$ we will use for the analysis the definition of the Caputo derivative (4): with the assumed profile (11) the function inside the fractional integral is $d^2 u_a(x, t)/dx^2 = [n(n-1)(1-x/\delta)^n] \delta^{-2}$. The Goodman boundary conditions (8) for $x \rightarrow \delta$ can be satisfied if $u_a(\delta, t) = \lim_{x \rightarrow \delta} (1 - x/\delta)^{n-2}$ that impose the requirement $n > 2$.

2.5.2 Evaluation of the truncated series expansions of $\Phi_0(n, \alpha, \beta)$, $\Phi_1(n, \alpha, \beta)$ and $\Psi(n, \alpha, \beta)$: additional constraint on the exponent n

The penetration depth contains the terms of $\Phi_0(n, \alpha, \beta)$, $\Phi_1(n, \alpha, \beta)$ and $\Psi(n, \alpha, \beta)$ and therefore the reasonable questions are :What the minimum value of n (at given α and β) is in order to assure the conditions $\Phi_0(n, \alpha, \beta > 0)$ and $\Phi_1(n, \alpha, \beta) > 0$. Answering to this question we have to take into account that $\Psi(n, \alpha, \beta) > 0$ because the value of δ is physically defined and positive by nature. Answers are given by Fig. 1a,b in case of ${}_{RL}\Phi_0(\alpha = 0, n, \beta)$ referring to the results reported in [42] for $D_{\beta 0} = const.$ where it established that 9 terms of the truncated series expansion are enough (the same was established in [43] when $D_{\beta} = D_{\beta 0} = x^{\alpha}$). The plots reveal that the variation of $\Phi_0(n, \alpha, \beta > 0)$ in a large interval of variation of n decreases as β increases. Now, the next step is to find the minimal values of n assuring $\Phi_0(n, \alpha, \beta > 0)$ using the already defined ranges of variations $n_{min} < n < n_{max}$ (see Fig. 1a,b).

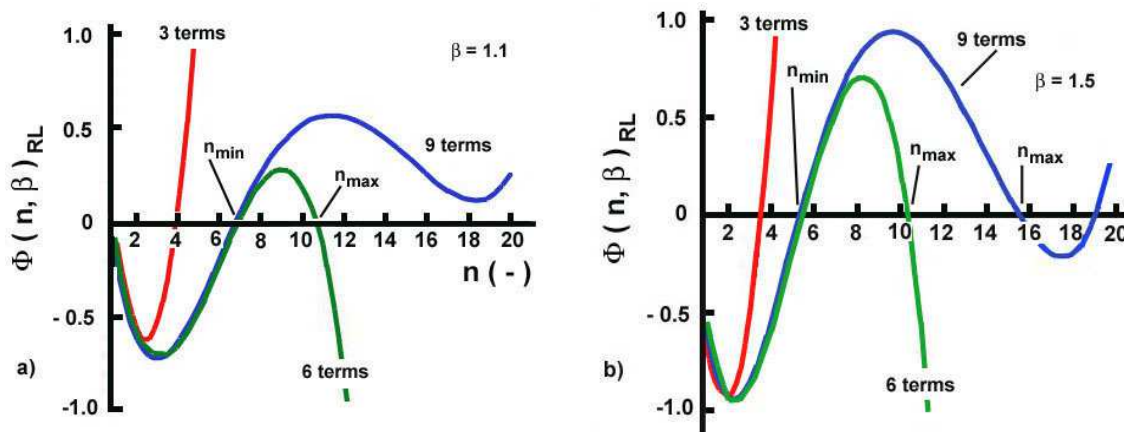


Fig. 1: Effect of the value of the exponent n on the variations of $\Phi_0(n, \alpha, \beta)$ and the number of terms of the truncated expansions of the assumed profile. Case for and two distinct values of the fractional order a) $\beta = 1$; b) $\beta = 1.5$

The numerical experiments presented in Fig. 2 clearly indicate that within the range of variation of $n(n_{min} < n < n_{max})$ for various $0 < \alpha < 1$ and $1 < \beta < 2$, we get $\Phi_1(n, \alpha, \beta) > 0$. It is noteworthy that within the same range of variations of n the positive branch of $\Psi(n, \alpha, \beta)$ is narrower (see Fig. 3), bounded by vertical asymptotes passing through the boundaries of the range of variations of n . Besides, these branches of the curve $\Psi(n, \alpha, \beta)$ exhibit minima with almost flat bottoms. These estimates allow to define approximately the range where the optimal values of the exponent n assuring minima of the residual functions should be searched for.

2.5.3 Order of magnitudes of $D_{\beta 0}$ and γ_x

Here we meet serious obstacles since the dominating published results [28, 32] are not related to real problems but mainly stress the attention on calculations. To avoid this problem and demonstrate feasibility of the developed approximate solutions we refer to some integer-order problems with spatially-varying diffusivity. Referring to the works of Hammed and Lebedeff [46], Voller [47] and others [48, 49, 50, 51] we stress attention that in most cases it is assumed $D_{\beta 0} \approx 1$ and $0 < \alpha < 1$ (which matches the preceding estimates in this work). Since ${}_sHr$ plays the role of the fractional Fourier number it is better to represent the approximate solutions in terms of the similarity variables $\xi_p = x / (D_{\beta 0} t)^{1/(\beta - \alpha)}$ (or $\xi_{pp} = x / (D_{\beta 0} t)^{1/\beta}$) and ${}_sHr$. If we assume $D_{\beta 0} = 1$ for simplicity and $t = 1$, then ${}_sHr = \gamma_x$. Further in this article we will use this simplified case to demonstrate how the optimal exponent of the approximate solution depends on α and β .

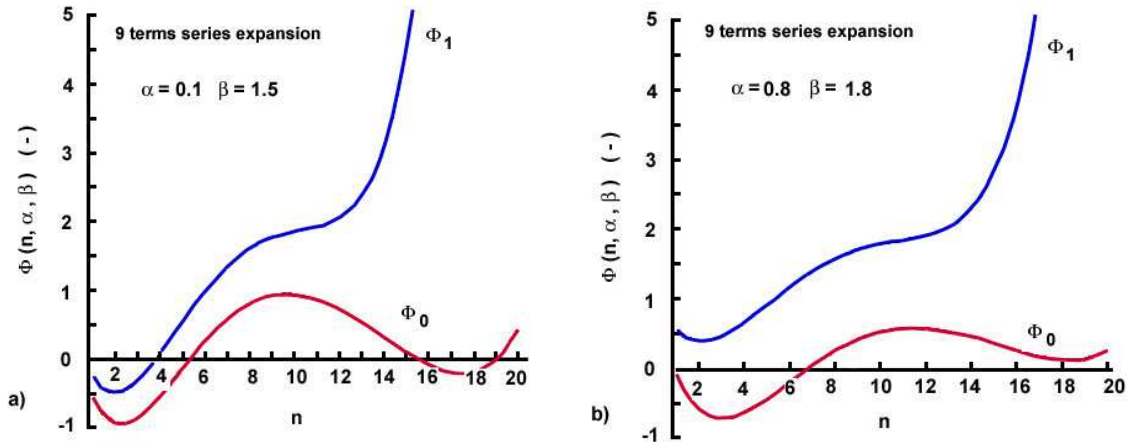


Fig. 2: Effect of the value of the exponent n on the variations of $\Phi_0(n, \alpha, \beta)$ and $\Phi_1(n, \alpha, \beta)$ as well as the number of terms of the truncated expansions of the assumed profile in two distinct cases a) $\alpha = 0.1$ and $\beta = 1.1$; b) $\alpha = 0.8$ and $\beta = 1.8$

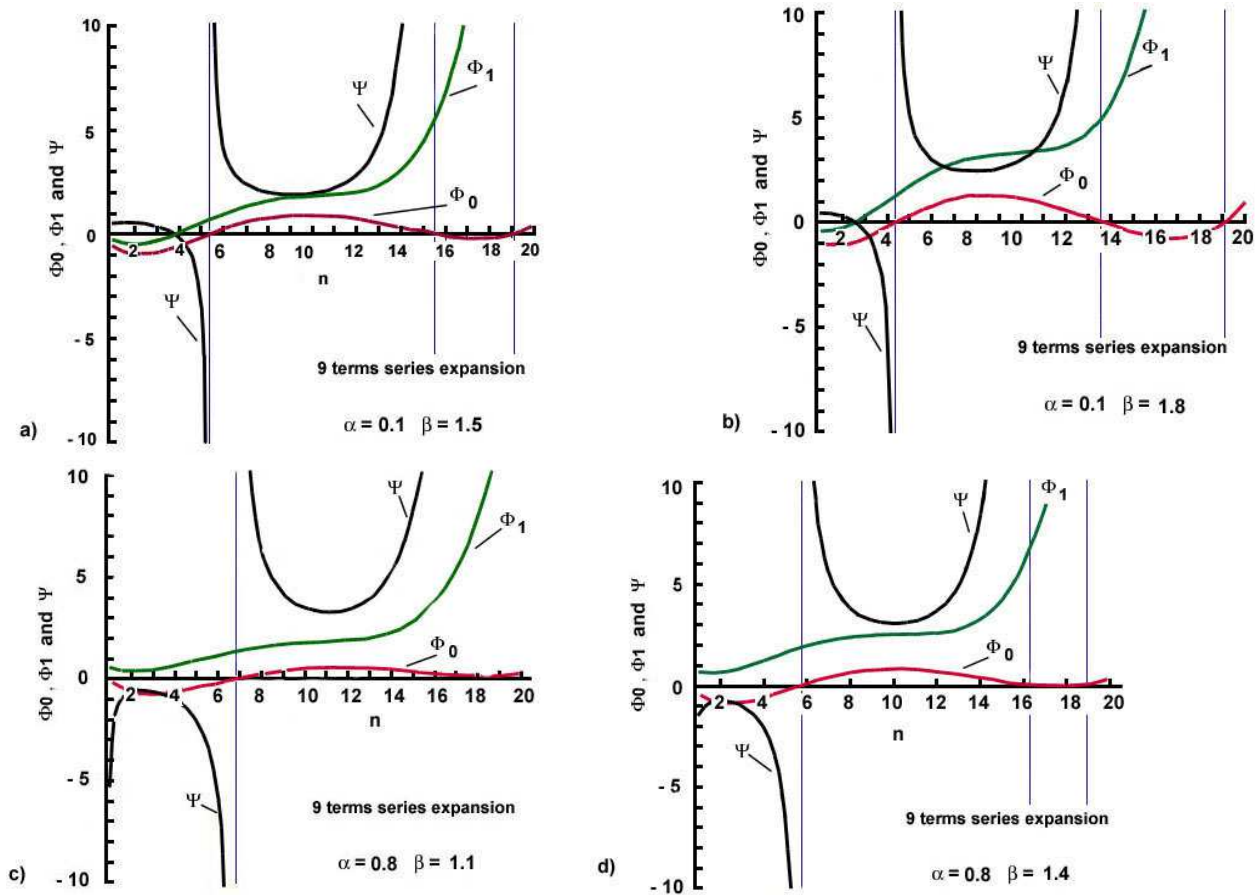


Fig. 3: Effect of the value of the exponent n on the variations of $\Phi_0(n, \alpha, \beta)$, $\Phi_1(n, \alpha, \beta)$ and $\Psi(n, \alpha, \beta)$ (9 terms truncated series expansion of u_a) and four distinct combinations of the exponent α and the fractional order β : (a) Case with $\alpha = 0.1$ and $\beta = 1.5$; (b) Case with $\alpha = 0.1$ and $\beta = 1.8$; (c) Case with $\alpha = 0.8$ and $\beta = 1.1$; (d) Case with $\alpha = 0.8$ and $\beta = 1.4$

2.6 Mean squared error of approximation and optimal exponents

The Langford criterion [52] for the integral-balance method can be defined as

$$E_L(n, \alpha, \beta, t) = \int_0^\delta (R(u_a(x, t)))^2 dx \longrightarrow \min. \tag{55}$$

In terms of the dimensionless variable η the integral in (55) can be expressed as

$$\int_0^1 \left(n(1-\eta)^{n-1} \frac{n}{\delta} \frac{d\delta}{dt} - D_{\beta 0} \delta^{-\beta} \frac{\partial^\beta F_a(\eta)}{\partial \eta^\beta} - \gamma_x \delta^{\alpha-\beta} \frac{\partial^\beta F_a(\eta)}{\partial \eta^\beta} \right) d\eta \longrightarrow \min. \tag{56}$$

Let us, for example, see what the expression of $E_{Lp}(\alpha, \beta)$ in the case of power-law diffusivity. From ((25) we have that $d\delta/dt = (n+1)\delta^{1+\alpha-\beta}\Phi_1(n, \alpha, \beta)$. Hence, with $\delta^{-1}d\delta/dt = (n+1)\delta^{\alpha-\beta}\Phi_1(n, \alpha, \beta)$ we can express eq.(56) as

$$E_L(n, \alpha, \beta, t) = (D_{\beta 0} \delta^{\alpha-\beta})^2 e_{Lp}(n, \alpha, \beta) \longrightarrow \min, \tag{57}$$

$$e_{Lp}(n, \alpha, \beta) = \int_0^1 [n(n+1)\Phi(n, \alpha, \beta)(1-\eta)^{n-1} - \eta^\alpha \frac{\partial^\beta F_a(\eta)}{\partial \eta^\beta}] d\eta. \tag{58}$$

Taking into account that $\delta^{\alpha-\beta} = t D_{\beta 0} (\beta - \alpha)(n+1)\Phi_1(n, \alpha, \beta)$ the way to ensure minimum error of approximation is to minimize with respect to n the second term of (57), i.e. $e_{Lp}(n, \alpha, \beta)$.

The error measure (57) can be presented as $E_L(n, \alpha, \beta) = e_L(n, \alpha, \beta)t^{-4}$, because the nominator gets in each term some of these products: $\delta^{-2}\delta_t^2 \equiv (1/t^4)$, $\delta^{2\beta} \equiv (t^{-2})$ and $\delta^{-(1+\beta)}\delta_t \equiv (t^{-2})$, while the denominator is proportional to $\delta^{-2\beta} \equiv (t^2)$. The estimation of the optimal n , minimizing $e_L(n, \alpha, \beta)$ was carried out in accordance with the following practically oriented scheme:

1. First, for given values of α and β , starting from an integer-order value of n within the range $n_{min} < n < n_{max}$ (see Fig.1 and Fig.2), not too close to the vertical asymptotes bounding $\Psi(n, \alpha, \beta)$ and 9 terms of the series expansions of $\Phi_0(n, \alpha, \beta)$ and $\Phi_1(n, \alpha, \beta)$ calculate the integral in (58) (by using Maple, for instance). The results will allow to calculate $e_L(n, \alpha, \beta)$.

2. Collecting all the data $e_L(n, \alpha, \beta)$ is it possible to create the functional relationship $e_L(n, \alpha, \beta)$ against n . Interpolation by as much as possible high-order polynomial will allow to define the minimum and therefore the optimal n . The optimal exponents defined in this way are presented in Table 1.

The values of optimal exponents reveal that they are independent of and but decrease with increase in , as it is illustrated in Fig. 4b (the same behavior was observed in [43] with $D_\beta(x) = D_{\beta 0 x^\alpha}$). The result could be attributed to the low impact of the second term (in the squared brackets) in the expressions for and which is proportional to and which in the range of variations of and have negligible effects on the penetration depth. In this context, the dependence of from is practically linear as it demonstrated in Fig.4c .

3 Numerical Experiments and Analyzes

3.1 Two-dimensional profiles and classification of the transport regimes

Approximate solutions as profiles expressed through the similarity variable ζ_1 are shown in Fig.5 and Fig.6. In general, they demonstrate that the increase in α results is larger values of δ that can be easily detected by the points where the profiles cross the abscissas.

The mean square displacement can be generalized as [53,54]

$$\langle x^2 \rangle = \int_0^\delta x^2 u(x, t) dx \propto t^{\frac{2}{d_w}}. \tag{59}$$

For $d_w = 2$ one classifies the diffusion process as follows [53,54,55,56]: *diffusion on fractal structure* is defined with $d_w > 2$, that is the transport is dispersive with reduced diffusion corresponding to the subdiffusion process because $\langle x^2 \rangle \propto t^{\frac{2}{d_w}}$ and $2/d_w < 1$; for $d_w = 2$ we have the Fickian diffusion. The case $d_w < 2$ indicates *enhanced diffusion* with the following sub-cases: for $1 < d_w < 2$ the transport regime is *intermediate*, for $d_w = 1$ there is a *ballistic transport* and for

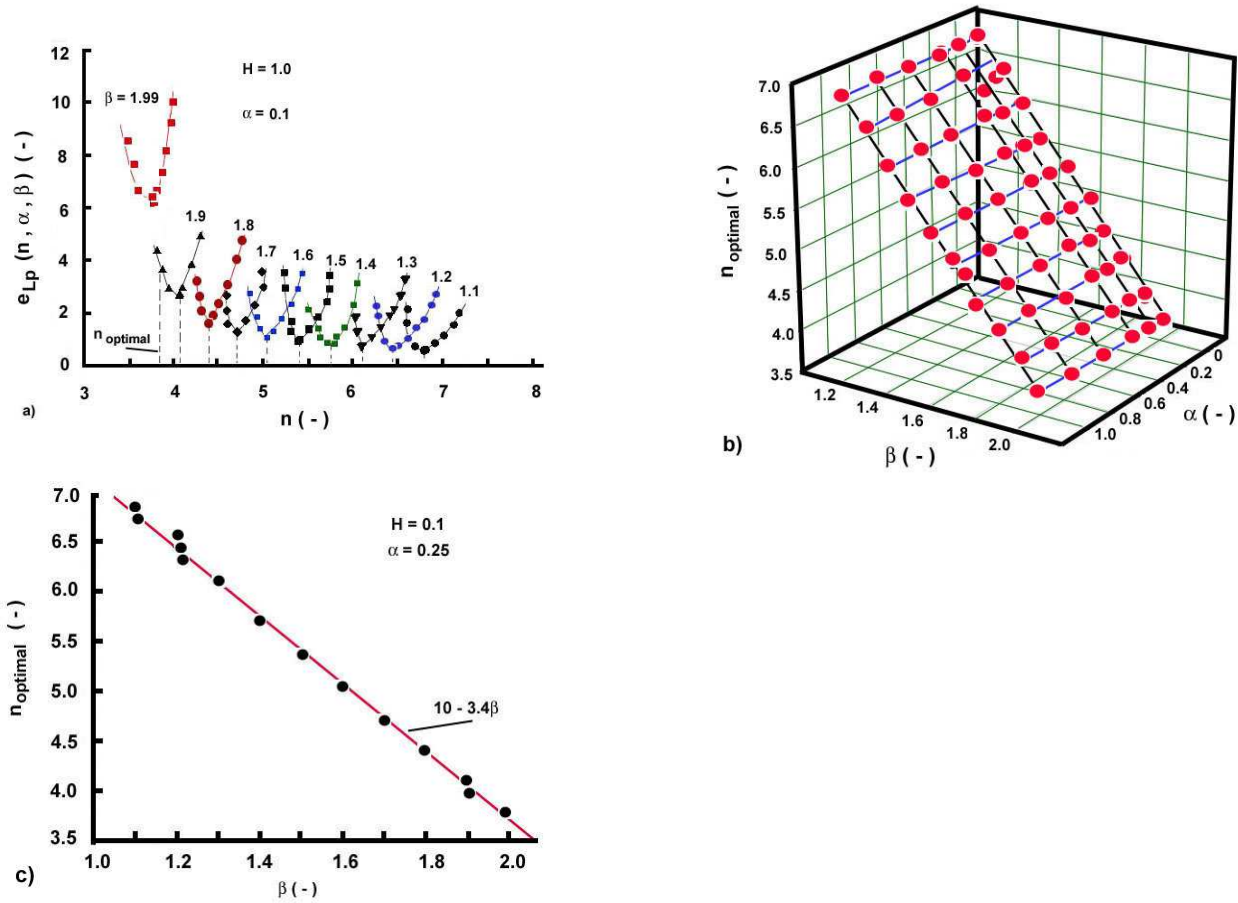


Fig. 4: Exponents determined by a minimization of the residual function. a) Residual functions around the minima for various values of the fractional order β . Demonstrative case for and $\alpha = 0.1$ and $sH_r = 1.0$. b) Three-dimensional scattered diagram $n_{opt} = f(\alpha, \beta)$. Case for $sH_r = 1.0$. c) Data correlation $n_{opt} = f(\beta)$ by a linear relationship. Case of $\alpha = 0.25$ and $sH_r = 0.1$. Due to the invariance of the values of n_{opt} with respect to the exponent α and sH_r , this correlation is valid for the entire ranges of the variations of the parameters studied in this article. **Note** :For the sake of simplicity the fractional Fourier number sH_r is denoted hereafter in the figures simply as H

$d_w < 1$ a turbulent transport takes place. The means squared displacement of the process at issue and with the approximate profile (8) is

$$\langle x^2 \rangle = \int_0^\delta x^2 \left(1 - \frac{x}{\delta}\right)^n dx = \frac{2\delta^2}{(n+1)(n+2)}. \tag{60}$$

With the assumed profile used in this work (see the expression about δ_2 for example) we get $\langle x^2 \rangle \equiv \delta^2 \propto t^{\frac{2}{\beta-\alpha}}$ (see the expression about δ_2 for example), that is difference $(\beta - \alpha)$ controls the process (see also [43] for similar results). It is worthy to stress the attention that irrespective of the expression about δ_1 or δ_2 the penetration depth is one and the same since it is physically defined quantity, that is $\delta_1 = \delta_2 = \delta$. Since $1 < \beta < 2$ in the case of $\delta_1^2 \propto t^{1/\beta}$ we have regimes of subdiffusion transports. This case confirms the results developed in [42] for $\alpha = 0$, therefore for $\gamma_x = 0$ and $D_\beta(x) = D\beta 0 = const$. Moreover, when the special diffusivity is represented by a simple power-law as [43] $D_\beta(x) = D\beta 0 x^\alpha$ we have $\delta^2 \propto t^{1/(\beta-\alpha)}$. Both cases where developed here in solution focusing on the penetration depth. Since the special diffusivity at issue is an additive function of this two simple cases it would be expected that their characteristic features will appear in the distribution of the approximate solutions along the abscissa (against the similarity variable ζ). The plots in Fig. 5 and Fig. 6 clearly demonstrate the effect of β in the arrangement of the curves from left to right but the effect

Table 1: Optimal exponents for various values of α , β and ${}_sH_r$

	β	1.1	1.2	1.3	1.4	1.5	1.6	1.7	1.8	1.9	1.99
		n_{opt}									
${}_sH_r$	$\alpha = 0$	6.823	6.490	6.082	5.691	5.381	5.076	4.708	4.411	4.003	3.780
0.001	$\alpha = 0.1$	6.780	6.329	6.084	5.728	5.380	5.039	4.707	4.381	4.064	3.784
0.01	$\alpha = 0.1$	6.780	6.447	6.084	5.728	5.380	5.039	4.706	4.381	4.064	3.785
1.0	$\alpha = 0.1$	6.780	6.447	6.090	5.729	5.380	5.039	4.706	4.381	4.064	3.785
10	$\alpha = 0.1$	6.780	6.447	6.084	5.728	5.380	5.040	4.708	4.386	4.064	3.785
	$\beta - \alpha$	1.0	1.1	1.2	1.3	1.4	1.5	1.6	1.7	1.8	1.88
0.001	$\alpha = 0.25$	6.818	6.570	6.084	5.728	5.380	5.039	4.707	4.381	4.064	3.784
0.01	$\alpha = 0.25$	6.818	6.447	6.084	5.727	5.380	5.039	4.710	4.381	4.070	3.785
1.0	$\alpha = 0.25$	6.780	6.447	6.090	5.729	5.380	5.039	4.707	4.381	4.064	3.785
10	$\alpha = 0.25$	6.780	6.447	6.084	5.728	5.380	5.040	4.708	4.386	4.064	3.785
	$\beta - \alpha$	0.85	0.95	1.05	1.15	1.25	1.35	1.45	1.55	1.65	1.74
0.001	$\alpha = 0.5$	6.818	6.447	6.084	5.728	5.345	5.039	4.707	4.381	4.064	3.785
0.01	$\alpha = 0.5$	6.818	6.447	6.084	5.728	5.351	5.039	4.707	4.381	4.064	3.785
1.0	$\alpha = 0.5$	6.818	6.447	6.084	5.728	5.376	5.039	4.707	4.381	4.064	3.785
10	$\alpha = 0.5$	6.818	6.447	6.084	5.728	5.346	5.039	4.707	4.381	4.064	3.785
	$\beta - \alpha$	0.6	0.7	0.8	0.9	1.0	1.1	1.2	1.3	1.4	1.49
0.001	$\alpha = 0.75$	6.818	6.447	6.084	5.728	5.380	5.039	4.707	4.381	4.064	3.784
0.01	$\alpha = 0.75$	6.818	6.447	6.084	5.728	5.380	5.039	4.707	4.381	4.064	3.785
1.0	$\alpha = 0.75$	6.818	6.449	6.084	5.728	5.380	5.100	4.707	4.381	4.063	3.784
10	$\alpha = 0.75$	6.818	6.449	6.084	5.728	5.380	5.039	4.707	4.3821	4.063	3.785
	$\beta - \alpha$	0.35	0.45	0.55	0.65	0.75	0.85	0.95	1.05	1.015	1.24
0.001	$\alpha = 1.0$	6.818	6.447	6.084	5.728	5.380	5.039	4.707	4.390	4.063	3.785
0.01	$\alpha = 1.0$	6.818	6.449	6.084	5.728	5.380	5.039	4.707	4.381	4.063	3.785
1.0	$\alpha = 1.0$	6.818	6.447	6.084	5.728	5.380	5.039	4.707	4.381	4.064	3.790
10	$\alpha = 1.0$	6.818	6.447	6.084	5.728	5.380	5.039	4.707	4.390	4.063	3.785
	$\beta - \alpha$	0.1	0.2	0.3	0.4	0.5	0.6	0.7	0.8	0.9	0.99

of α is not obvious and therefore we have the answer the question: why the order of arrangements the profiles changes in both sides of the point $\beta - \alpha = 1$? To answer this question it is better to use the alternative case $\delta_2 \propto t^{2/(\beta-)}$.

For $\beta - \alpha < 2$, which encompass all cases studied here we have enhanced diffusion with the following sub-cases [53, 54, 55, 56], namely: for $1(-\alpha) < 2$ the transport regime is *intermediate*, for $(\beta - \alpha) = 1$ there is a *ballistic transport* and for $(\beta - \alpha) < 1$ a *turbulent transport* takes place. Now, the data summarized in Table 1 allows identifying that:

For $\alpha = 0$ and $\alpha = 0.1$ we have $0 < (\beta - \alpha) < 2$ and all profiles are propagating faster with increase in the fractional order β thus corresponding to the *intermediate transport* regime .

For $\alpha = 1$ in all cases $0 < (\beta - \alpha) < 1$ the profiles correspond to the *turbulent transport* regime.

Intermediate values of α there is a change in the transport mechanism depending on the value of β , namely

$$\alpha = 0.25, 1.3 < \beta < 1.9 \implies 1 < (\beta - \alpha) < 2$$

$$\alpha = 0.5, 1.5 < \beta < 1.9 \implies 1.5 < (\beta - \alpha) < 2$$

$$\alpha = 0.75, 1.8 < \beta < 1.8 \implies 1 < (\beta - \alpha) < 2$$

Using these estimations we state that with increasing in α the process shifts from the *intermediate* to the *turbulent* regime, and *vice versa*. In the present study there are two cases corresponding to $(\beta - \alpha) = 1$, i.e. ($\alpha = 0.1$ and $\beta = 1.1$) and ($\alpha = 0.5$ and $\beta = 1.5$). As commented earlier, in these cases the fronts propagate with constant speeds.

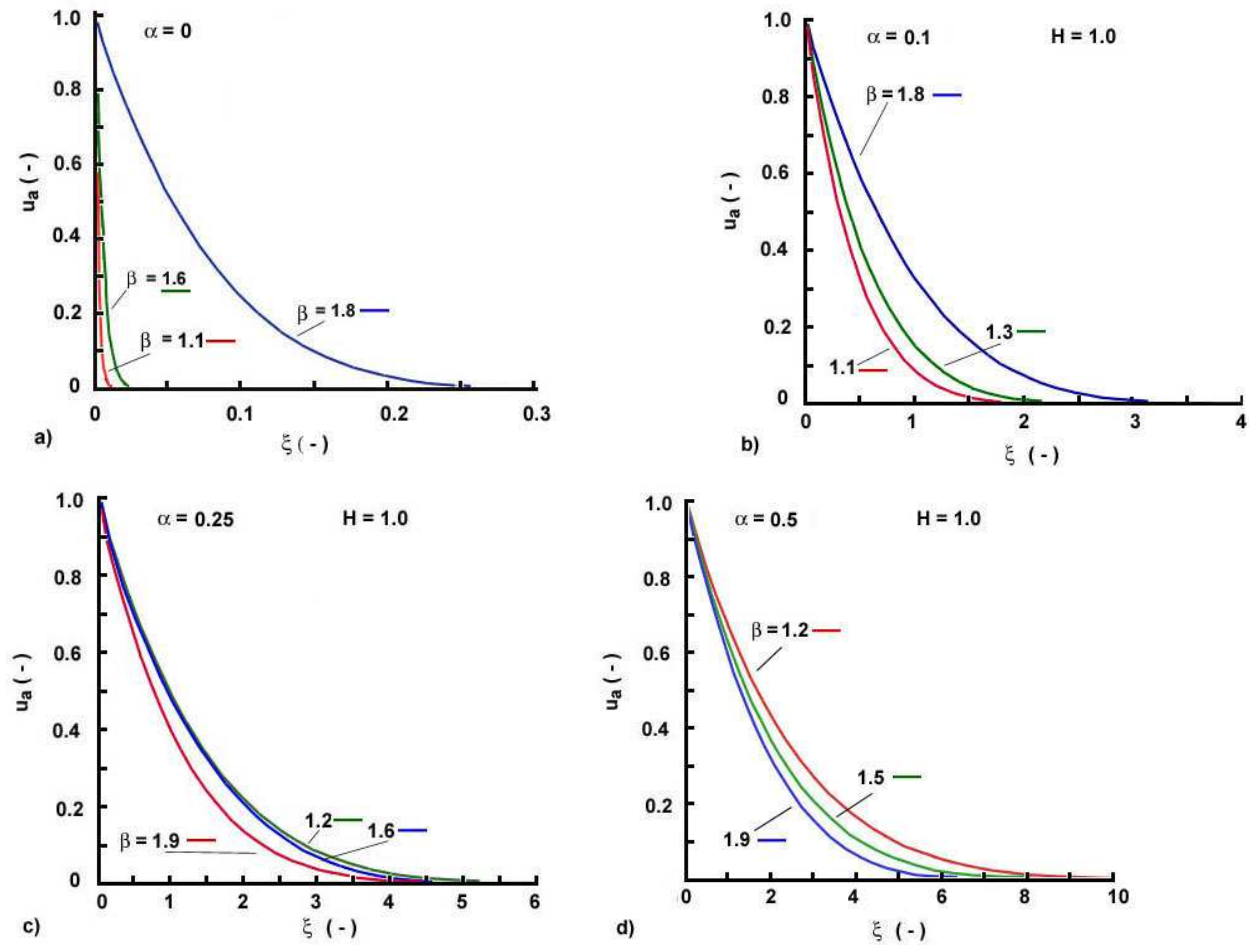


Fig. 5: Approximate two-dimensional profiles. Situations when the order of arrangement of the profiles along the abscissa follows the decrease in the fractional order β corresponding to the range $0 \leq \alpha \leq 0.5$. The case corresponds to intermediate and turbulent transport regimes (see the comments in the text). Case of ${}_sH_r = 1.0$. a) $\alpha = 0$; b) $\alpha = 0.1$; c) $\alpha = 0.25$; d) $\alpha = 0.5$

A good example is the solutions for $\alpha = 0.5$, where the transport mechanism for $\beta < 1.5$ is different from that for $\beta > 1.5$ although the arrangement of the curves follows the same order as that exhibited by the solution for cases with $\beta - \alpha < 1$, precisely the cases for $\alpha = 0.75$ and $\alpha = 1$ correspond to the *turbulent transport*.

All these transients from one transport mechanism to another strongly depends on the difference $\beta - \alpha$ and affect the arrangement of the approximate profiles along the abscissa, as commented above. More clear explanations come up from the three-dimensional presentation of the approximate solution commented in the next section.

3.2 Three-dimensional profiles and evolution of $\delta(t)$ with respect to β and $(\beta - \alpha)$

Three-dimensional presentations of the approximate solution in the form $ua = f(\xi, \beta, \alpha = const., {}_sH_r = const.)$ are shown in Figs. 7, 8, 9 and 10. The optimal exponent n_{opt} was approximated as a function of the fractional order β as $n_{opt} = 10 - 3.4\beta$ (see Fig. 4c.) since it is practically independent of the exponent α .

It is noteworthy that fixed value of the dimensionless number ${}_sH_r$ means a fixed moment of time scaled by the characteristic time (t_1 or t_2). Hence, when similarity variable is used as available along the axis ξ , in fact, this is a scaled axis of the coordinate x at fixed moment of time. Now, after these preliminary explanation let us see the solution at different times and the effect of the difference $\beta - \alpha$.

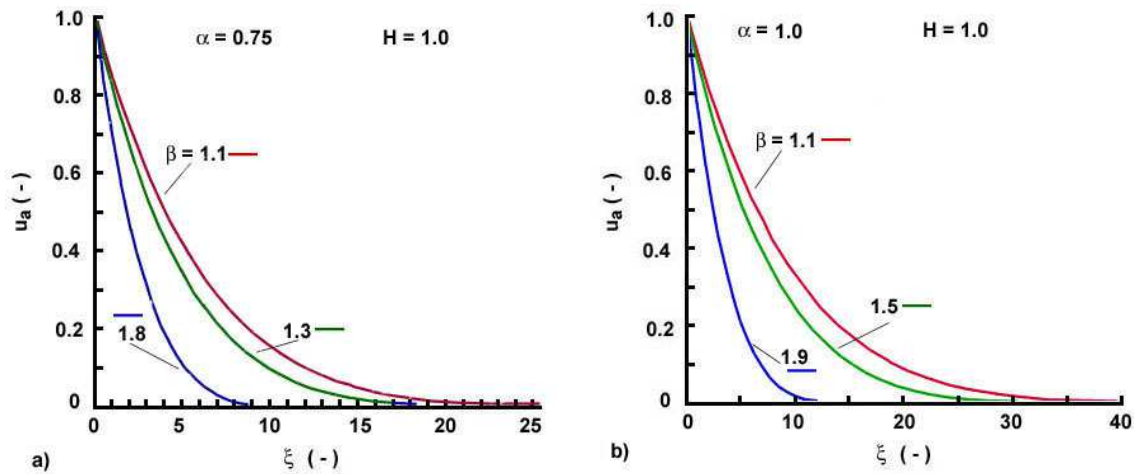


Fig. 6: Approximate two-dimensional profiles. Situations when the order of arrangement of the profiles along the abscissa do not follow exactly the decrease in the fractional order β corresponding to the range $0.75 \leq \alpha \leq 1.0$, that is almost linear dependence $D_{\beta 0}(x) = f(x)$ (see the comments in the text). Case of ${}_s H_r = 1.0$. a) $\alpha = 0.75$; b) $\alpha = 1.0$

3.2.1 Small, moderate and large time solutions

The three-dimensional representations of the approximate solutions in Fig. 7 and Fig. 8, represents cases of small (${}_s H_r = 0.1$) and moderate (${}_s H_r = 1$) times. The envelope $\delta(t)$ shows the front propagation and its variation along the β axis. In general, for $\alpha < 0.5$ the short time solutions correspond to $\delta < 4\xi$ and we have an envelope $\delta(t)$, concave in shape with respect to the β axis. The increase in the area between the line $\delta(t)$ and the β axis corresponding to the cases where $-\alpha < 1$ makes the envelope more concave. To clarify this statement, let see the large time solutions represented by the case when ${}_s H_r = 5$ (see Fig.9) and ${}_s H_r = 10$ (see Fig.10) but for $\alpha < 0.5$ as in these shown in Fig. 7 and Fig. 8. The increase in time makes the envelope $\delta(t)$ convex in shape (with respect to the β axis. It is easy to detect differences in $\delta(t)$ when β varies from 1 to 2 and the effect of the difference $\beta - \alpha$. Looking at the meaning of the fractional order β the slowest case when $\beta = 2$ corresponds to the classical diffusion equation and the shorter penetration depth $\delta(t)$, respectively. The reduction in the values of β transforms the governing equation to a model corresponding to faster transport regimes with a limit when $\beta = 1$ with the largest $\delta(t)$. Therefore, the solutions and they behaviours when the controlling fraction order β varies are physically adequate.

3.2.2 Almost linear and linear relationship $D_{\beta}(x)$

It is interesting to see the solution behaviour when $D_{\beta}(x) = D_{\beta 0} + \gamma x^{\alpha}$ approaches the linear relationship. Two cases for $\alpha = 0.75$ and $\alpha = 1$ are presented in Fig.11 and Fig. 12 respectively. In these cases the increase in time (from the top of the column of sub-figures to the bottom) indicates concave $\delta(t)$ profiles with respect to the β axis. For the linear case ($\alpha = 1$) we can clearly see the retardation (forcing) effect of α since in all these cases ($0.1 \leq {}_s H_r \leq 10$) we have $\beta - \alpha < 1$ except the limiting situation with $\beta = 2$ and consequently the front propagation is as $\delta(t) \propto t^1 / (\beta - \alpha)$ where $1 / (\beta - \alpha) > 1/2$, that completely corresponds to superdiffusive transport $1 / [(\beta - \alpha)]^2 > 1$. The solutions with the lower value of $\alpha = 0.75$ in Fig. 11 encompass cases with $\beta - \alpha < 1$ and $\beta - \alpha > 1$ ($\beta > 1.75$) and the simultaneous effect of the fractional order β and the exponent α .

4 Conclusions

This paper reported approximate analytical solution of transient space-fractional diffusion (Dirichlet problem) by a synergistic combination of the integral-balance method, which in fact allows solving the problem by the two-point method, and the least-squares approach allowing defining the optimal exponent of the assumed profile. Precisely, the

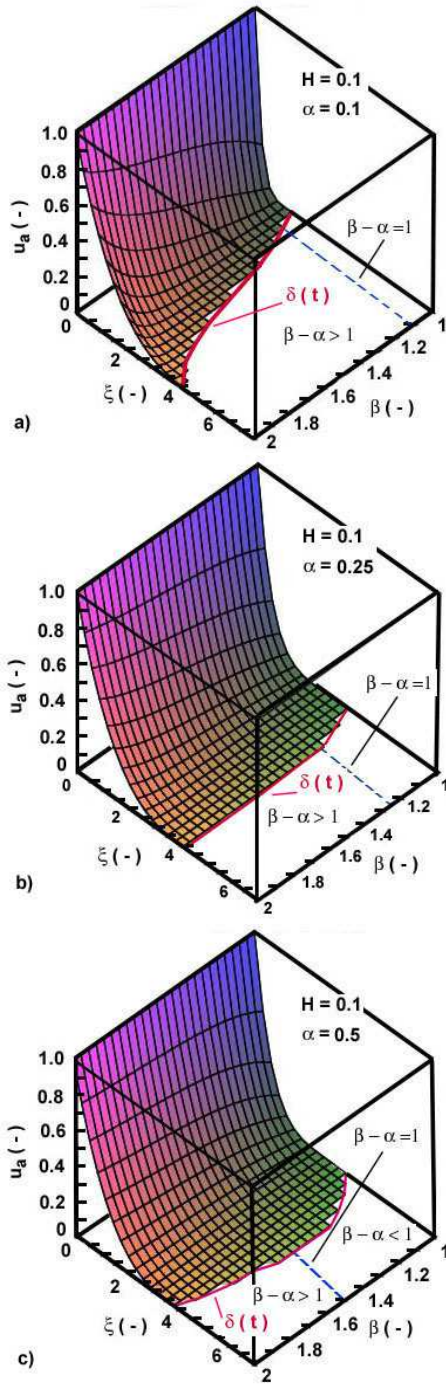


Fig. 7: Three-dimensional approximate profiles (solutions) for small times ($sH_r = 0.1$) as a function of the exponent α and the fractional order β demonstrating the effect of the difference $(\beta - \alpha)$ on the shape of the advancing front $\delta(t)$ (the red line in the web version) within the range $0 \leq \alpha \leq 0.5$. **Note:** the line is hand-made drawn demonstrating only the tendency in variation of the front $\delta(t)$.

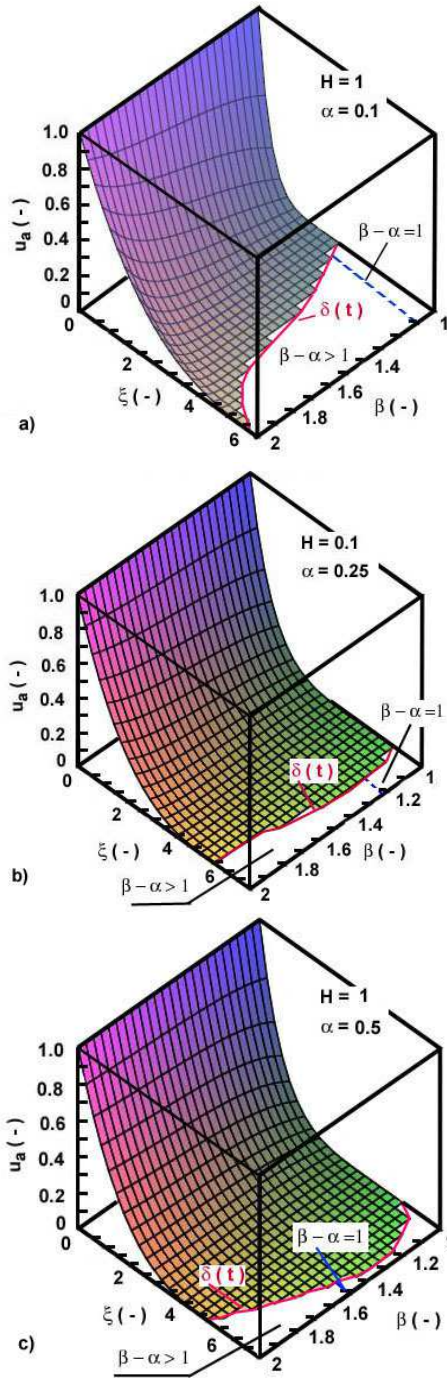


Fig. 8: Three-dimensional approximate profiles (solutions) for moderate times ($sH_r = 1.0$) as a function of the exponent α and the fractional order β demonstrating the effect of the difference $(\beta - \alpha)$ on the shape of the advancing front $\delta(t)$ (the red line in the web version) within the range $0 \leq \alpha \leq 0.5$. **Note:** the line is hand-made drawn demonstrating only the tendency in variation of the front $\delta(t)$.

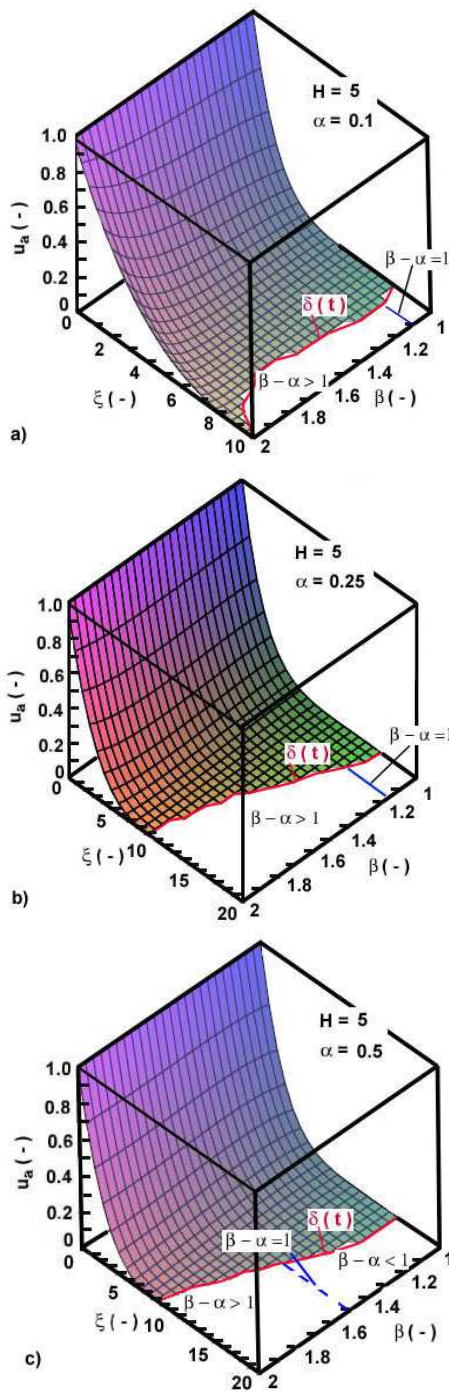


Fig. 9: Three-dimensional approximate profiles (solutions) for large times (${}_sH_r = 5$) as a function of the exponent α and the fractional order β demonstrating the effect of the difference $(\beta - \alpha)$ on the shape of the advancing front $\delta(t)$ (the red line in the web version) within the range $0 \leq \alpha \leq 0.5$. **Note:** the line is hand-made drawn demonstrating only the tendency in variation of the front $\delta(t)$.

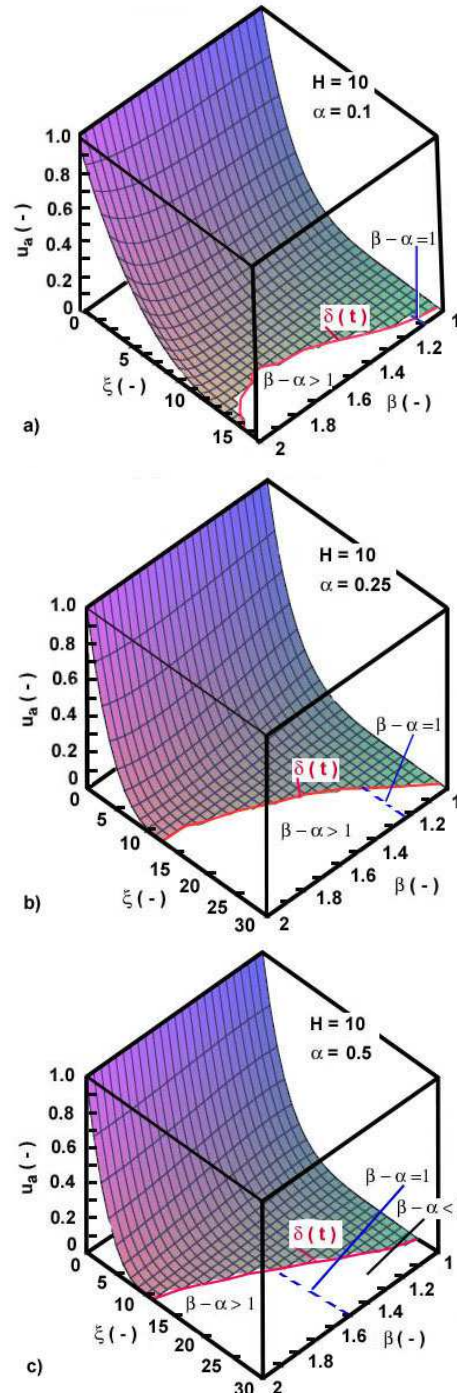


Fig. 10: Three-dimensional approximate profiles (solutions) for large times (${}_sH_r = 10$) as a function of the exponent α and the fractional order β demonstrating the effect of the difference $(\beta - \alpha)$ on the shape of the advancing front $\delta(t)$ (the red line in the web version) within the range $0 \leq \alpha \leq 0.5$. **Note:** the line is hand-made drawn demonstrating only the tendency in variation of the front $\delta(t)$.

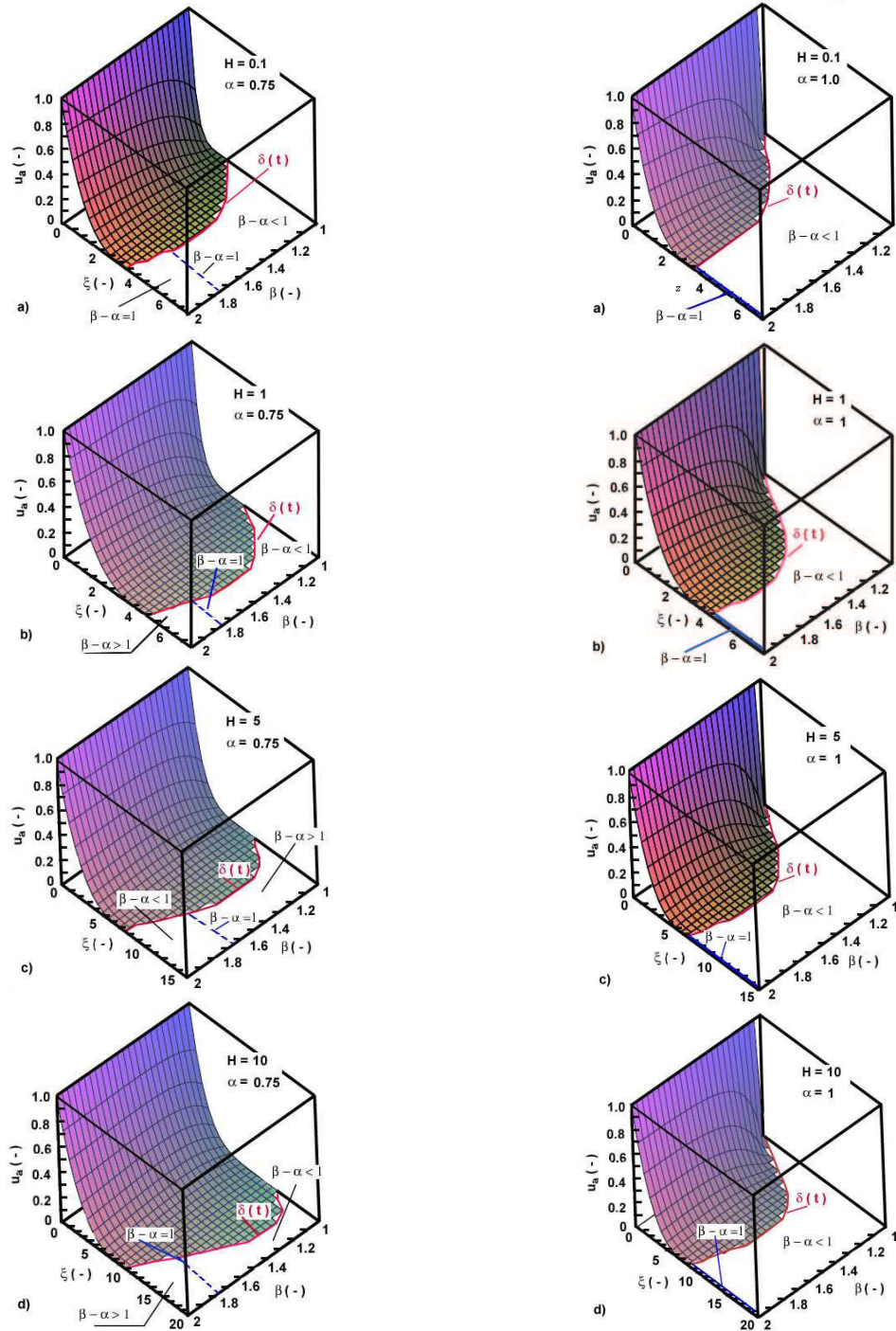


Fig. 11: Three-dimensional approximate profiles (solutions) for almost linear functional relationship $D\beta(x) = f(x)$ ($\alpha = 0.75$) as a function of the exponent α and the fractional order β demonstrating the effect of the difference $(\beta - \alpha)$ on the shape of the advancing front $\delta(t)$ (the red line in the web version) within the range $0 \leq \alpha \leq 0.75$. From top to the bottom of the column the time increases (increased values of sH_r) **Note:** the line is hand-made drawn demonstrating only the tendency in variation of the front $\delta(t)$

Fig. 12: Three-dimensional approximate profiles (solutions) for almost linear functional relationship $D\beta(x) = f(x)$ ($\alpha = 1.0$) as a function of the exponent α and the fractional order β demonstrating the effect of the difference $(\beta - \alpha)$ on the shape of the advancing front $\delta(t)$ (the red line in the web version) within the range $0 \leq \alpha \leq 0.75$. From top to the bottom of the column the time increases (increased values of sH_r) **Note:** the line is hand-made drawn demonstrating only the tendency in variation of the front $\delta(t)$

front functional relationship, termed here as penetration depth is developed by the single-integration approach of the integral-balance method. The refining of the approximate solution that is the determination of the optimal exponent uses the least-squares approach by minimization of the residual function of the governing equation. Further, the assumed parabolic profile expansion as a convergent power-law series allows easily applying either integer-order or fractional-order differentiation and integrations.

The solution reveals that the front propagation depends on the inverse of the difference of the fractional order β and spatial exponent of the diffusion coefficient α thus allowing transitions from subdiffusive to superdiffusive transport regime.

The optimal exponent of the approximate profile is practically independent of the spatial exponent of the diffusion coefficient but it is strongly affected by the fractional order β demonstrating almost linear relationship; the optimal exponent decreases with increase in the fractional order β . The three-dimensional presentation of the results permits to demonstrate the effect of the difference of the fractional order β and spatial exponent of the diffusion coefficient α . Moreover, the potential power-law spatial relationship of the diffusion coefficient conceived in this article results in definition of the fractional Fourier number controlling the process. This allowed demonstrating the effect of the fractional Fourier number on the development of the approximate solution at short, moderate and large times.

References

- [1] J. J. Trujillo, *Fractional models: Sub and super-diffusive, and undifferentiable solutions*, In: B. H. V.Topping, G. Montero, and R.Montenegro (Eds). *Innovation in Engineering Computational Technology*. Sax-Coburg Publ., Stirling, UK, 2006, pp. 371–402.
- [2] R. R. Nigmatullin, The realization of the generalized transfer equation in a medium with fractal geometry, *Phys. Stat. Sol. (B) Basic Research* **133**, 425–430 (1986).
- [3] O. G. Bakunin, Description of the anomalous diffusion of fast electrons by a kinetic equation with a fractional spatial derivative, *Plasma Phys. Rep.* **30**, 338-342 (2004).
- [4] O. G. Bakunin, Diffusion equations and turbulent transport, *Plasma Phys. Rep.* **29**, 955–970 (2003).
- [5] Y. Luchko and H. M. Srivastava, The exact solution of certain differential equations of fractional order by using operational calculus, *Comp. Math. Appl.* **29**, 73–85 (1995)
- [6] J. H. He, Approximate analytical solution for seepage flow with fractional derivatives in porous media, *Comp. Meth. Appl. Mech. Eng.* **167**, 57–68 (1998).
- [7] R. Y. Molliq, M. S. M. Noorani and I.Hashim, Variational iteration method for fractional heat and wave like equations, *Nonlinear Anal. Real World Appl.* **10**, 1854–1869 (2009).
- [8] J. Nakagawa, K. Sakamoto and M. Yamamoto, Overview to mathematical analysis for fractional diffusion equations new mathematical aspects motivated by industrial collaboration, *J. Math. Ind.* **2**, 99-108 (2010A-10).
- [9] S. Das, P. K. Gupta and P. Ghosh, An approximate analytical solution of nonlinear fractional diffusion equation, *Appl. Math. Mod.* **35**, 4071–4076 (2011).
- [10] G. C. Wu, Variational iteration method for solving the time-fractional diffusion equations in porous medium, *Chin. Phys. B.* **21**, Article ID 120504 ; doi: 10.1088/1674-1056/21/12/120504 (2012).
- [11] G. C. Wu, Applications of the variational iteration method to fractional diffusion equations: local versus nonlocal Ones, *Int. Rev. Chem. Eng.* **4**, 505-510 (2012).
- [12] G. C. Wu and D. Baleanu, Variational iteration method for fractional calculus—a universal approach by Laplace transform, *Adv. Differ. Equ.* **2013**, doi:10.1186/1687-1847-2013-18 (2013).
- [13] F. Liu, S. Shen, V. Anh and I. Turner, Analysis of a discrete non-Markovian random walk approximation for the time fractional diffusion equation, *Anziam J.* **46**, 488–504 (2004).
- [14] F. Liu, P. Zhuang, V. Anh, I. Turner and K. Burrage, Stability and convergence of the difference methods for the space-time fractional advection-diffusion equation, *Appl. Math. Comput.* **191**, 12–20 (2007).
- [15] P. Zhuang and F. Liu, Implicit difference approximation for the time fractional diffusion equation, *J. Appl. Math. Comput.* **22**, 87–99 (2006).
- [16] M. M. Meerschaert and C. Tadjeran Finite difference approximations for two-sided space-fractional partial differential equations, *Appl. Numer. Math.* **56**, 80–90 (2006).
- [17] T. S. Basu and H. Wang, Fast second-order finite difference method for space-fractional diffusion equations, *Int. J. Numer. Anal. Mod.* **9**, 658–666 (2012).
- [18] I. Podlubny, *Fractional Differential Equations*, Academic Press, New York, 1999.
- [19] V. J. Ervin, N. Heur and J. Roop Numerical approximation of a time dependent, nonlinear, spacefractional diffusion equation, *SIAM J. Num. Anal.* **45**, 572–591(2008).
- [20] C. P. Li, Z. G. Zhao and Y. Q. Chen Numerical approximation of nonlinear fractional differential equations with subdiffusion and superdiffusion, *Comp. Math. Appl.* **62**, 855–875 (2011).
- [21] A. Saporita, P. Corneti and A. Carpinteri, Diffusion problems on fractional nonlocal media, *Centr. Eur. J. Phys.*, **11**, 1255-1261 (2013).

- [22] M. El-Kady, S. M. El-Sayed and S. E. El-Gendi Analysis of a discrete non-Markovian random walk approximation for the time fractional diffusion equation, *Anziam J.* **46**, 488–504 (2004).
- [23] Y. Zheng and Z. Zhao, A fully discrete Galerkin method for a nonlinear space-fractional diffusion equation, *Math. Probl. Engin.* **2011**, Article 171620, 20 pages.
- [24] A. Saadatmandi and M. Deghan, A tau approach for solution of the space fractional diffusion equation, *Comp. Math. Appl.* **62** (2011), 1135–1142.
- [25] N. Nie, J. Huang, W. Wang and Y. Tang, Solving spatial-fractional partial differential diffusion equations by spectral method, *J. Stat. Comp. Sim.* **84**, 1173–1189 (2014).
- [26] S. S. Ray, A new approach for the application of Adomian decomposition method for the solution of fractional space diffusion equation with insulated ends, *Appl. Math. Model.* **202**, 544–549 (2008).
- [27] S. S. Ray, Analytical solution for the space fractional diffusion equation by two-step Adomian decomposition method, *Comp. Nonlin. Sci. Num. Simul.* **14**, 1295–1306 (2009).
- [28] S. S. Ray, K. S. Chaudhuri and R. K. Bera, Application of modified decomposition method for the analytical solution of space fractional diffusion equation, *Appl. Math. Comput.* **196**, 294–302 (2008).
- [29] F. Huang and F. Liu, The space-time fractional diffusion equation with Caputo derivatives, *J. Appl. Math. Comput.* **19**, 179–190 (2005).
- [30] F. Huang and F. Liu, The fundamental solution of the space-time fractional advection-diffusion equation, *J. Appl. Math. Comput.* **19**, 339–350 (2005).
- [31] J. F. G. Aguilar and M. M. Hernandez, Space-time fractional diffusion-advection equation with Caputo derivative, *Abstr. Appl. Anal.* **2014**, Article ID 283019, 8 pages. Doi: 10.1155/2014/283019.
- [32] A. Fabre and J. Hristov, On the integral-balance approach to the transient heat conduction with linearly temperature-dependent thermal diffusivity, *Heat Mass Tran.* in press, doi: 10.1007/s00231-016-1806-5 (2016).
- [33] M. H. Cobble, Non-linear heat transfer in solids in orthogonal coordinate systems, *Int. J. Nonlin. Mech.* **2**, 417–4126 (1967).
- [34] J. Sucec and S. Hedge, Transient conduction in slab with temperature dependent thermal conductivity, *Transaction ASME* **100**, 172-174 (1978).
- [35] S. H. Lin, Transient heat conduction with temperature-dependent thermal conductivity by the orthogonal collocation method, *Lett. Heat Mass Tran.* **5**, 29–39 (1978).
- [36] N. Noda, Thermal stresses in materials with temperature dependent properties, IN: G.A.Schneider, G., Petzow (Eds.), *Thermal shock and thermal fatigue behaviour of advanced ceramics*, Nato Science Series, **241**, 15-26, Kluwer Academics Publ., Berlin, 1993.
- [37] T. R. Goodman, Application of integral methods to transient nonlinear heat transfer, In: Irvine TF and Hartnett JP (Eds.), *Adv. Heat Tran.*, **1**, 51–122, Academic Press, San Diego, CA, 1964.
- [38] J. Hristov, The heat-balance integral method by a parabolic profile with unspecified exponent: Analysis and benchmark exercises, *Therm. Sci.* **13**, 22–48 (2009).
- [39] J. Hristov, Heat-balance integral to fractional (half-time) heat diffusion sub-model, *Therm. Sci.* **14**, 291–316 (2010).
- [40] J. Hristov, Approximate solutions to fractional subdiffusion equations: The heat-balance integral method, *Eur. Phys. J. ST.* **193**, 229–243 (2011).
- [41] J. Hristov, Approximate solutions to time-fractional models by integral balance approach. In: C. Cattani, H. M. Srivastava, X. J. Yang (Eds.), *Fractals and Fractional Dynamics*, 78–109, De Gruyter Open, Berlin, 2015.
- [42] J. Hristov, An approximate solution to the transient space-fractional diffusion equation: Integral-balance approach, optimization problems and analyzes, *Therm. Sci.*, in press, DOI:10.2298/TSCI160113075H (2016).
- [43] J. Hristov, Transient space-fractional diffusion with a power-law superdiffusivity: Approximate integral-balance approach, *Fundam. Inform.*, in press (2016).
- [44] K. B. Oldham and J. Spanier *The fractional calculus*, Academic Press, New York, USA, 1974.
- [45] J. Hristov, Double integral-balance method to the fractional subdiffusion equation: Approximate solutions, optimization problems to be resolved and numerical simulations, *J. Vibr. Contr.*, in press, doi: 10.1177/1077546315622773.
- [46] S. Hamed and S. A. Lebedeff, Application of the integral method to heat conduction in nonhomogeneous media, *J. Heat Tran.* **97**, 304–305 (1975).
- [47] V. Voller, Analytical models of solidification phenomena, *Trans. Indian Inst. Met.* **62**, 279–283 (2009).
- [48] G. Liu and B.C. Si, Analytical modeling of one-dimensional diffusion in layered systems with position dependent diffusion coefficients, *Adv. Water. Res.* **31**, 251–168 (2008).
- [49] A. J. Kassab and E. Divo, A generalized boundary integral equation for isotropic heat conduction spatially varying thermal conductivity, *Eng. Anal. Bound. Elem.* **18**, 273–286 (1996).
- [50] M. Goharkhah, S. Amiri and H. Shokouhmand, Effect of spatial variation of thermal conductivity on non-Fourier heat conduction in a finite slab, *J. Mech. Sci. Tech.* **23**, 3393–3998 (2009).
- [51] Y. Pachepsky and D. Timlin, Water transport in soils as in fractal media, *J. Hydr.* **(204)**, 98–107 (1998).
- [52] D. Langford, The heat balance integral method, *Int. J. Heat Mass Tran.* **16**, 2424–2428 (1973).
- [53] M. O. Vlad, R. Metzler, T. F. Nonnenmacher and M. C. Mackey, Universality classes for asymptotic behavior of relaxation processes in systems with dynamical disorder: Dynamical generalization of stretched exponentials, *Math. Phys.* **37**, 2279–2301 (1966).
- [54] G. Baumann, N. Sudland and T. F. Nonnenmacher, Anomalous relaxation and diffusion processes in complex systems, *Transp. Theor. Stat. Phys.* **29**, 151–171 (2000).

- [55] K. S. Fa and E. K. Lenzi, Time-fractional diffusion equation with time dependent diffusion coefficient, *Phys. A* **72** article 011107 (2005), doi:10.1103/PhysRevE.72.011107.
- [56] K. S. Fa and E. K. Lenzi Power law diffusion coefficient and anomalous diffusion: Analysis of solutions and the first passage time, *Phys. Rev. E* **67**, article 061105 (2003), doi: 10.1103/PhysRevE.67.061105.
-